Firoozy, N., Mojabi, P., Landy, J., & Barber, D. G. (2016). Landfast First-Year Snow-Covered Sea Ice Reconstruction via Electromagnetic Inversion. *IEEE Journal of Selected Topics in Applied Earth Observations and Remote Sensing*, *9*(6), 2414-2428. [7420544]. https://doi.org/10.1109/JSTARS.2016.2525858

Seasonal dynamics of algal and bacterial communities in Arctic sea ice under variable snow cover

K. Campbell,[1]✉

Email umcampb2@myumanitoba.ca

C. J. Mundy,[1]

C. Belzile,[2]

A. Delaforge,[1]

S. Rysgaard,[1,3,4]

[1] Faculty of Environment, Earth and Resources, Centre for Earth Observation Science, University of Manitoba, Winnipeg, MB, R3T 2N2 Canada

[2] Institut des sciences de la mer de Rimouski, Université du Québec à Rimouski, Rimouski, QC, G5L 3A1 Canada

[3] Department of Bioscience, Arctic Research Centre, University of Aarhus, C.F. Møllers Allé 8, 1110, 213, 8000 Aarhus C, Denmark

[4] Greenland Institute of Natural Resources, Kivioq 2, 3900 Nuuk, Greenland

Abstract

The abundance of diatoms and heterotrophic bacteria in sea ice rapidly increases during the spring. However, the number and activity of these microorganisms vary with changing environmental conditions and potentially the taxonomic composition of the algal community during this time. In this study, we assessed the spring bottom-ice community composition in Dease Strait, Nunavut, and investigated potential controls of chlorophyll *a* (chl *a*), particulate organic carbon (POC), cell abundance, and production from early March until early June. We found that using flow cytometry to estimate photosynthetic nanoeukaryotes~~s~~remove the plural (2–20 µm) abundance gave results very similar to light microscopy

counts, except when pennate diatoms with lengths close to 20 μm, the maximum size detected by flow cytometry, were abundant. Using the average abundance of nanoeukaryotes from the two methods, we documented a change in the size of cells comprising the ice algal community over the spring, from largely pico- (<2 μm), to nano- and microeukaryotes (20–200 μm). This shift in ice algal size corresponded to a bloom in diatoms that drove increases in chl *a*, POC, and primary productivity. Low-salinity surface waters, limited nutrient availability, as well as seasonally intensifying light in the bottom ice appeared to support dominance of the centric diatom *Attheya* spp. Increases in the number and productivity of heterotrophic bacteria in this study were correlated with the number of photosynthetic picoeukaryote cells, potentially due to their supply of dissolved organic carbon substrate. Our results suggest that future conditions predicted for the Arctic that include low nutrients and greater light transmission to the bottom of sea ice may favor an ice algal community dominated by centric diatoms versus the more characteristic pennate diatom-dominated community.

Keywords

Arctic
Sea ice
Diatoms
Bacteria
Flow cytometry
Light microscopy

Electronic supplementary material

The online version of this article (doi:10.1007/s00300-017-2168-2) contains supplementary material, which is available to authorized users.

Introduction

Sea ice is a habitat for microbial life, particularly for algae and heterotrophic bacteria that are concentrated in the bottommost centimeters of the brine network and along the surface of ice crystals at the growth interface (Smith and Clement 1990; Deming 2010, Hawes et al. 2012). The abundance of ice algae and bacteria during spring in the Arctic increases rapidly with favorable growth conditions, namely the availability of light for algal photosynthesis (Gosselin et al. 1985; Lee et al. 2008; Søgaard et al. 2010) and the abundance of dissolved organic carbon (DOC)

for bacterial production (Haecky and Anderson 1999; Søgaard et al. 2013). The ice algal bloom is marked by an increase in the quantity of chlorophyll *a* (chl *a*) and particulate organic carbon (POC) in the ice, where the ice algae provides a concentrated food resource for aquatic grazers (Søreide et al. 2010). The type of algae comprising biomass in the ice is also an important consideration, as the nutritional value of different species varies and can impact grazer succession (Li et al. 2009; Leu et al. 2011). Furthermore, the majority of ice algae are consumed once detached from the ice (Michel et al. 1996), and variable sinking rates among species could impact ice–pelagic–benthic coupling as a result.

AQ1

Bacterial and algal production influences carbon fluxes through the ice and contributes to the overall productivity of the marine system, by releasing or consuming CO_2, respectively (Søgaard et al. 2010). Ice algae account for the majority of production during the spring and typically represent between 3 and 60% of total primary production in the Arctic Ocean (Legendre et al. 1992; Gosselin et al. 1997), while bacteria contribute <10% of the total production in sea ice (Deming 2010). Autotrophic cyanobacteria also have the potential to influence production; however, they have only been documented in trace quantities and their contribution to sea ice production is likely to be insignificant as a result (Mundy et al. 2011; Bowman 2015) .

The ice algal bloom in Arctic first-year sea ice is largely composed of pennate diatoms of the nano- (2–20 µm)- and micro- (20–200 µm)-size classes (Mendle and Priddle 1990; Lee et al. 2008; Różańska et al. 2009). This includes the typically dominant cryophilic microeukaryote *Nitzschia frigida* (Różańska et al. 2009; Poulin et al. 2011), which is nutritionally valuable to grazers due to high polyunsaturated fatty acid (PUFA) content (Leu et al. 2011). Other groups of morphologically similar protists are also present including centric diatoms, dinoflagellates, flagellates, and ciliates ~~are also present~~ (Mendle and Priddle 1990; Niemi et al. 2011), although the relative contribution of each group to the sea ice community varies with environmental conditions (Kirst and Wiencke 1995). For example, flagellates can outcompete diatom groups in the ice when photosynthetically active radiation (PAR) is severely restricted (Mikkelsen et al. 2008; Różańska et al. 2009). The presence of picoeukaryotic cells (<2 µm) in sea ice is not well understood, but recent studies have suggested that auto-, mixo-, and heterotrophic picoeukaryotes can be numerous in the ice (Piwosz et al. 2013).

Primary production in sea ice is largely controlled by the intensity of light reaching the bottom ice (Michel et al. 2002; Campbell et al. 2016), which is inversely related to the thickness of snow cover on the ice surface, and by nutrient supply from the water column (Gosselin et al. 1985; Cota and Horne 1989). The photosynthetic state of algae is species specific, where different taxa can exhibit varying rates of photoacclimation or respiration in response to changing environmental conditions like growth light intensity (Falkowski and Owens 1978). It follows that shifts in the taxonomic composition of the bottom-ice algal community that have been observed over the spring (e.g., Hsaio 1992; Mikkelsen et al. 2008; Niemi et al. 2011) could influence primary productivity through varied photosynthetic responses of different taxa to environmental conditions (Kirst and Wienke 1995). The size classification of the algal community may also have a significant effect on production, as smaller cells can be more productive relative to their biomass than larger cells due to their faster turnover rates (Agawin et al. 2000).

Bacteria follow similar distributions to algae over time and space in the sea ice because the majority of DOC required for bacterial production is sourced from the ice algae (e.g., Rysgaard and Glud 2004; Comeau et al. 2013). Other factors have also been suggested to affect bacterial abundance and production in sea ice including the number of bacterivores like choanoflagellates (Sime-Ngando et al. 1997; Riedel et al. 2007; Deming 2010), temperature, and cell lysis following viral infection (Maranger et al. 2015). Quantifying the impact of these controls on bacteria is required to better understand variability in bacterial production that is observed across the Arctic (Bunch and Harland 1990; Maranger et al. 1994; Kaartokallio et al. 2013) and the role of sea ice in the microbial food web (Sarmiento and Gruber 2006).

In this study, we describe the composition of the microbial community in the bottom centimeters of first-year sea ice over the spring bloom, under comparatively high and low light conditions that are characteristic of thin and thick snow covers, respectively. This includes quantifying the abundance of bacteria and individual size classes (pico-, nano-, and micro-) of eukaryotic algae using a combination of flow cytometry and inverted light microscopy, and documenting the taxonomic composition of algal cells. We also compare estimates of nanoeukaryote abundance from these methods in an effort to evaluate the use of flow cytometry in sea ice research. Finally, we discuss how environmental conditions in sea ice may control the community of microorganisms and indirectly affect chl *a*, POC, and gross primary production.

Materials and methods

Sample collection

Different sample sites of thin (<10 cm) and thick (15–25 cm) snow-covered sea ice were chosen approximately every 4 days in Dease Strait, Nunavut (Fig. 1), between 7–15 March and 21 April–9 June. The bottom 5 cm of six to eight ice cores was collected under both thin and thick snow covers, using a 9-cm Mark II Kovacs core barrel. Ice samples from each site were pooled together before melting in darkness over 24 h with 0.2 μm filtered seawater (FSW, filtered within 48 h of collection) and added at a volumetric ratio of three parts FSW to one part ice melt. The resulting ice–FSW solution of pooled cores was used for all measurements of pooled cores hereafter. Estimates from these samples reported per unit of volume (abundance, productivity, etc.) have been multiplied by the ratio of total volume (FSW + ice melt) to ice melt, to account for core dilution. Volume estimates (mL^{-1}) may be converted to per unit area (m^{-2}) by applying an additional multiplication factor of 50,000. A separate ice core was taken under thin snow cover to measure the temperature and bulk salinity in the bottom 5 cm of sea ice. Please refer to Campbell et al. (2016) for additional information.

Fig. 1

a Location of sample collection in the Canadian Arctic, with **b** average snow (*black*) and ice (*gray*) thickness over the study period shown for sites designated as thin and thick

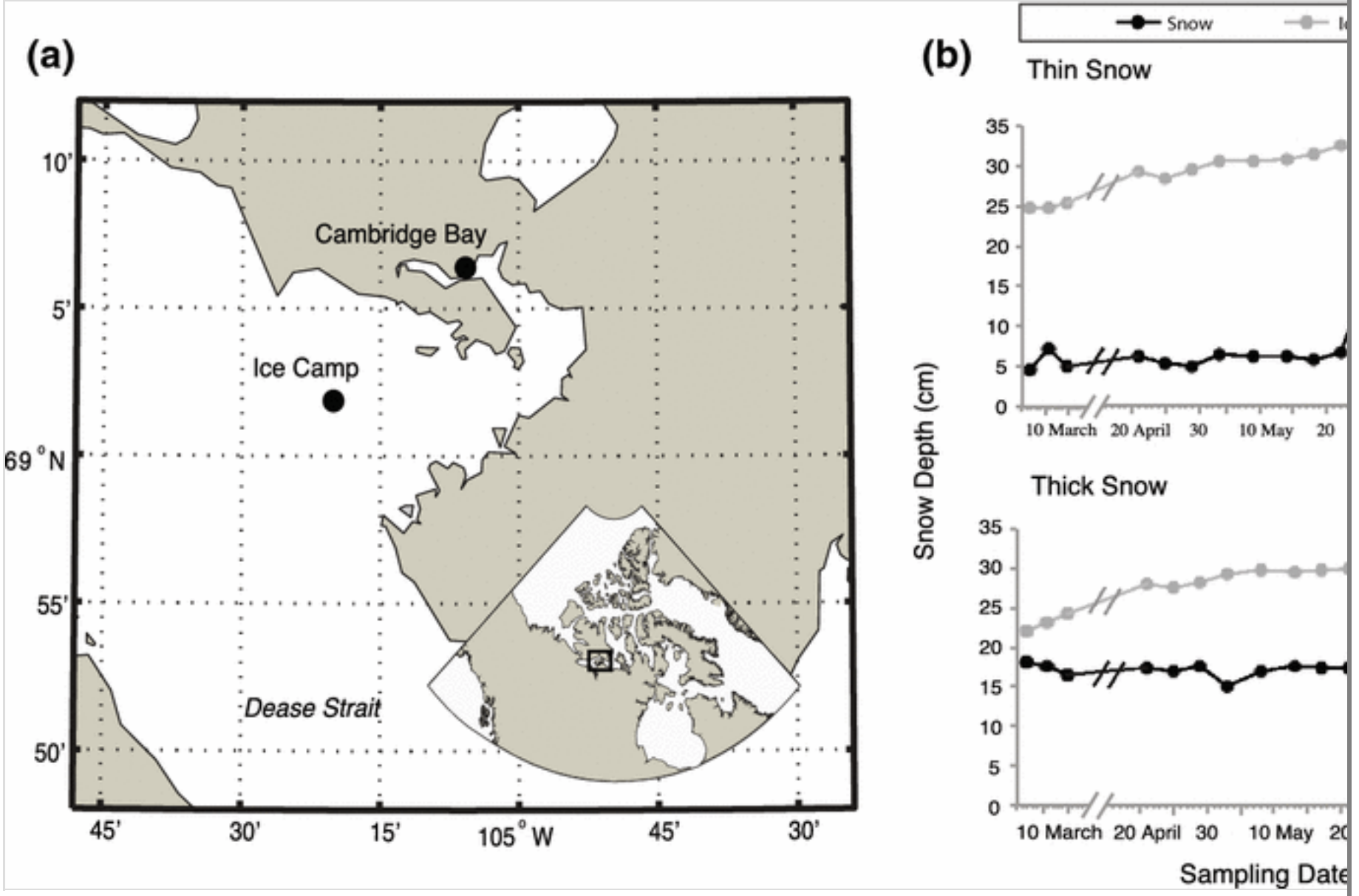

Measurements of photosynthetically active radiation (PAR)

The intensity of downwelling PAR at the ocean–ice interface [E_z(PAR)] was measured opportunistically over the sampling period under thin and thick snow covers and is reported for the respective core collection dates by averaging estimates on, or within, ±2 days of ice core collection (except for the 21 April sampling event). Measurements were made between 9:00 and 12:30 local time using 2π quantum sensors (LI-COR) and a mechanical arm (Campbell et al. 2016). Incident downwelling PAR above the snow and ice cover was also recorded at a nearby meteorological tower using a *Kipp & Zonen PAR-Lite* sensor and is presented as a daily average.

Biological parameters

Chlorophyll *a* and POC were sampled from the pooled cores by filtration through unburned and precombusted GF/F filters (*Whatman*), respectively. Chlorophyll *a* concentration was determined in the field using fluorescence (*Turner Designs Trilogy* Fluorometer; Parsons et al. 1984), while POC filters were frozen until later analysis using a continuous-flow isotope ratio mass spectrometer (*Thermo Scientific*)

following Glaz et al. (2014). The concentration of nitrate (NO_3) and nitrite (NO_2) was determined by filtering a volume from a separate ice core that was not diluted with FSW through precombusted GF/F filters (Whatman). The filtrate was stored at −20 °C and later analyzed on an auto analyzer (Seal Analytical) for nitrate (NO_3) and nitrite (NO_2), collectively referred to as NO_x, according to Strickland and Parsons (1972). The concentration of NO_x was also measured on water collected from the ocean–ice interface following this method. Measurements of DOC were done on interface water samples by filtering pseudo-duplicate 8-mL samples through precombusted GF/F filters into glass vials that were previously washed in 10% HCl for 24 h and burned for 12 h at 450 °C. Samples were immediately acidified with 100 µL 2-N HCl, closed with acid-washed caps, and stored at 4 °C in darkness until analysis on a high-temperature combustion total organic carbon analyzer (Shimadzu TOC-V_{cpn}). Salinity of interface water was recorded (Orion Star A212 conductivity meter) and is reported here as a dimensionless quantity.

Bacterial and primary production

Bacterial production was calculated from a 6-h dark incubation of pooled ice core sample (15 mL) with 10 nM concentration of ^{3}H-leucine, following Kirchman (2001). Triplicate blanks were fixed with trichloroacetic acid (TCA, 5% final concentration) prior to incubation, and triplicates of active vials were fixed with TCA immediately afterwards. Samples were filtered through 0.2-µm cellulose acetate membranes that were dissolved with 0.5 mL ethyl acetate prior to 24–48 h of extraction in EcoLume scintillation cocktail (5 mL) and measurement of activity on a liquid scintillation counter (*Hidex Triathler*). Bacterial production (g C l^{-1} h^{-1}) was calculated using equations outlined in Kirchman (1993) and a carbon conversion factor of 1.5 kg C mol^{-1} leucine (Ducklow et al. 2003).

Estimates of daily primary production were calculated using photosynthetic parameters described in Campbell et al. (2016) that were measured on the same pool of ice cores described above. Therefore, measurements of production were made on all size classes of algae present in a given sample. Primary production was only measured from 21 April to 9 June (n = 12). Diurnal estimates of under-ice PAR required for the calculation of production were determined by applying the average PAR transmittance under thin (2.2%) and thick (1.7%) snow sites in Campbell et al. (2016) (Online Resource 1), to hourly averages of downwelling PAR measured at the meteorological station [E_0(PAR)].

Flow cytometry

Pseudo-duplicate samples of 4.5 mL were taken from the melted pool of ice cores for later assessment of algal and bacterial cell abundance using a flow cytometer. Samples were fixed with glutaraldehyde at a final concentration of 0.4% immediately after collection, before storage at −80 °C for up to 6 months. They were analyzed using an Epics Altra flow cytometer (*Beckman Coulter*) following the protocols outlined in Tremblay et al. (2009) to determine the abundance of photosynthetic picoeukaryotes (<2 μm), nanoeukaryotes (2–20 μm). and cyanobacteria, and protocols of Belzile et al. (2008) to count heterotrophic bacteria.

Light microscopy

Subsamples of 100 mL from the pooled ice cores were fixed with acidic lugol (Parsons et al. 1984) for enumeration of visible cells (>2 μm) and taxonomic analysis, which was completed within one year of collection using an inverted light microscope (Leica DMIL LED). The abundance of cells per milliliter was adjusted to account for core dilution (see "Sample collection" section). Ice algae were identified to the lowest possible taxonomic rank, mainly using Poulin and Cardinal (1982), Medlin and Priddle (1990), and Tomas (1997) for reference. Based on morphological similarities, cells were assigned to the protist groups of pennate diatoms, centric diatoms, dinoflagellates, ciliates, or others, similar to Niemi et al. (2011). The abundance of nanoeukaryotic cells (exclusive of choanoflagellates) and microeukaryotes was estimated following this assessment by summing cell counts of taxa that are not known to exceed or are typically greater than 20 μm in length (see Online Resources 3, 4 for specific taxa designations). Additional information on light microscopy methods is detailed in Online Resource 1.

Estimates of relative abundance

The relative abundance of algae within each size class (i.e., pico-, nano-, micro-) was determined by calculating the percent of each class relative to the sum of picoeukaryotic cells measured with flow cytometry, the average nanoeukaryotic abundance from flow cytometry and light microscopy, and the number of microeukaryotes estimated from light microscopy. The percent composition of protist groups was assessed relative to the total number of classified cells counted with light microscopy, including the 'other group' that represented <0.5% of cell abundance in all samples. Unidentified cells from light microscopy were not included in estimates of absolute or relative abundance for either size or taxonomic

analyses, as they could not be defined as protists with certainty.

Statistical analyses

The SPSS (IBM Version 20) software was used for all statistics presented. This includes Student's paired *t* tests to assess differences or similarities between thin and thick snow covers (reported with the test statistic and sample size as t_n), and Pearson correlation statistics (r) to assess linear trends. The average values reported in this research are reported with (±) standard deviations and sample size (n).

Results

Study site and environmental conditions

Information on the physical characteristics of the field site from April to June is described in detail by Campbell et al. (2016). Here we summarize conditions inclusive of March sampling, while additional information can be found in Online Resource 2. The study site was covered by a drifted snowpack for the duration of sampling, with snow cover averaging 6.4 ± 1.6 cm under thin sites, and 17.7 ± 2 cm under thick sites (n = 14, exclusive of 26 May) (Fig. 1). This difference in snow depths resulted in significantly higher E_Z(PAR) under thin snow (paired *t* test, $t_{13} = 5.908$, $p < 0.0001$) (Fig. 2a). A late spring snowfall caused unseasonably low measurements of E_z(PAR) on 5 and 9 June, and analysis hereafter uses estimates of under-ice PAR downwelling between 7 March and 30 May only. Transmitted PAR data inclusive of June sampling dates are differentiated by E_z(June) where applicable. Salinity measured at the ice–ocean interface was stable during the spring (April–June) at 28.1 ± 0.2 (n = 24) (Campbell et al. 2016). This salinity is relatively fresh compared to surface waters elsewhere in the Arctic Ocean (Jackson et al. 2011; Campbell et al. 2016).

Fig. 2

Seasonal change in **a** downwelling of PAR averaged daily at the snow–ice surface [E_0(PAR)] (*dashed*) and measured at the ice–ocean interface [E_z(PAR)] (*solid*) with standard deviation *(*n = 3), **b** bottom-ice chlorophyll *a* (chl *a*) with standard deviation (n = 2) from Campbell et al. (2016), and **c** bottom-ice particulate organic carbon (POC) concentrations. With the exception of downwelling PAR at the surface, estimates were made on ice covered by thin (*black*) and thick (*gray*) snow covers

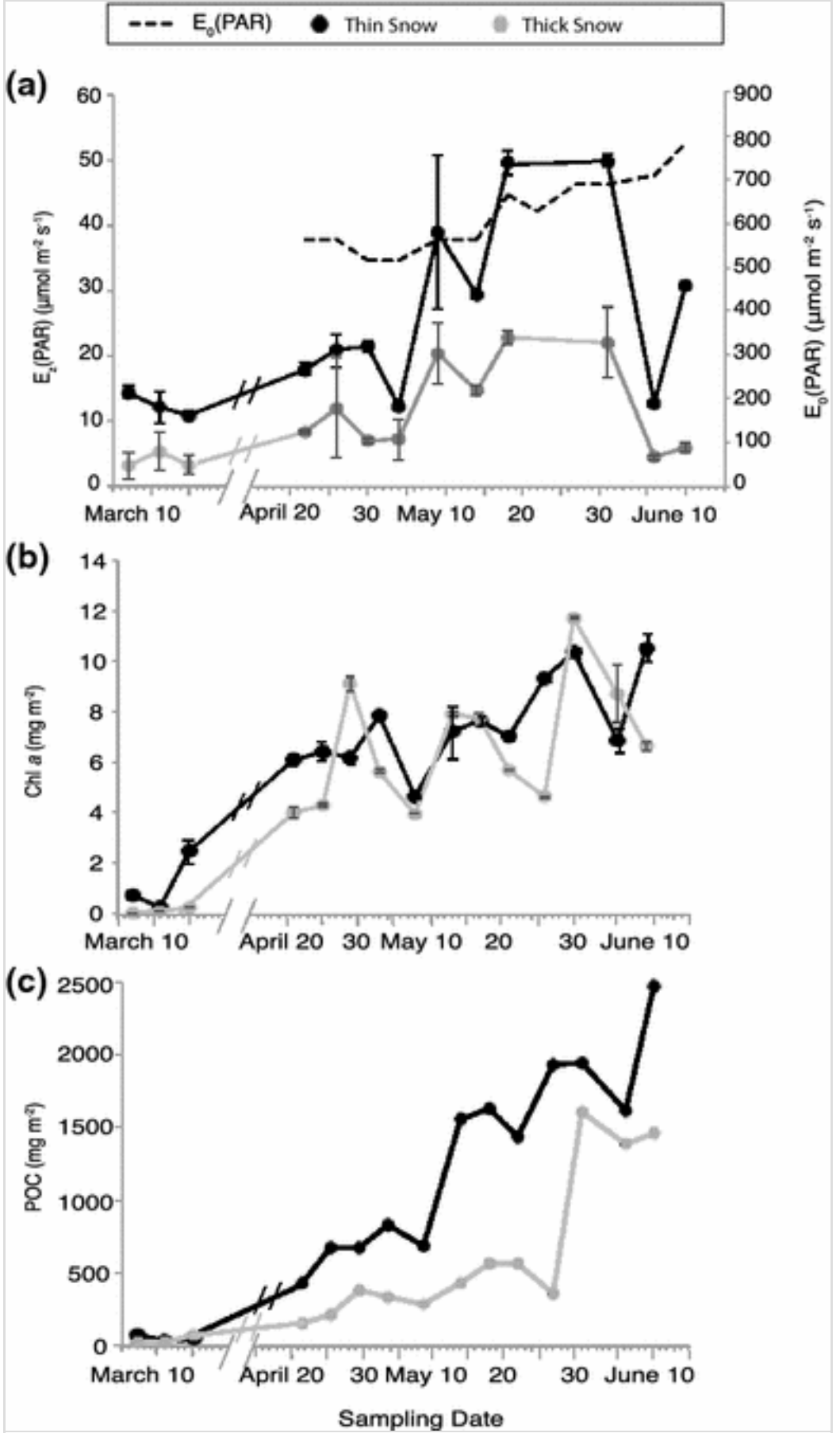

The concentration of chl *a* in the bottom ice increased over the spring under thin ($r = 0.898$, $p < 0.0001$, $n = 15$) and thick snow ($r = 0.821$, $p = 0.0002$, $n = 15$) (Fig. 2b). Chlorophyll *a* was not statistically different between thin and thick snow covers (paired *t* test, $t_{15} = 1.662$, $p = 0.119$), averaging 6.3 ± 3.1 mg m^{-2} under thin snow and 5.4 ± 3.5 mg m^{-2} under thick snow ($n = 15$). Particulate organic carbon in the sea ice also increased between 7 March and 9 June under thin ($r = 0.907$, $p < 0.0001$, $n = 15$) and thick ($r = 0.782$, $p = 0.001$, $n = 15$) snow, although the maximum concentration of POC under thick snow (1606 mg m^{-2}) was reached on 30 May (Fig. 2c). Particulate organic carbon was highest under thin snow (paired *t* test,

$t_{15} = 4.423$, $p = 0.001$), averaging 1069 ± 779 mg m^{-2}, versus 526 ± 525 mg m^{-2} under thick snow ($n = 15$). The concentration of DOC in seawater collected from the ocean–ice interface was largely constant over the spring at 1.9 ± 0.3 mg C L^{-1} ($n = 15$), with the exception of 7 March where the measurements reached 3 mg C L^{-1} (data not shown).

There are inherent problems associated with the collection of ice nutrient data, and their representation of nutrient availability for sea ice algae. It is beyond the scope of the current study to investigate these shortcomings, but we stress that bulk ice nutrients presented represent a proxy for nutrient availability. Furthermore, we have not corrected measurements of bulk ice nutrients for salinity, but the reader may adjust values at their discretion using the stable ratio of brine to bulk ice salinity calculated in Campbell et al. (2016) of 3.1 ± 0.6 ($n = 12$).

The average concentration of NO_x in the bottom ice was 0.61 ± 0.44 µmol L^{-1} under thin and 0.86 ± 0.51 µmol L^{-1} under thick snow ($n = 15$). Concentrations decreased from 7 March to 9 June largely under thin snow ($r = -0.713$, $p = 0.003$, $n = 15$), rather than thick snow ($r = -0.269$, $p = 0.332$, $n = 15$), due to greater ice algal demand (Campbell et al. 2016). The concentration of NO_x in surface water immediately beneath the ice was relatively constant over the spring at 1.17 ± 0.3 µmol L^{-1} ($n = 15$). Both NO_x concentrations in the bottom ice and interface water were low compared to other regions of the Arctic, and were found to limit algal photosynthesis during the study period (Campbell et al. 2016). Please refer to Campbell et al. (2016) for details on nutrient-limited conditions in Dease Strait, and the resulting impact on algal photophysiology, composition, and production.

Heterotrophic bacterial abundance and production

The abundance of heterotrophic bacteria in the bottom ice reached maximum concentrations on 8 May at 10×10^6 cells mL^{-1} under thin snow and 6.5×10^6 cells mL^{-1} under thick snow (Fig. 3a). Cell abundance was fairly constant after this date, at a lower average concentration of $2.4 \times 10^6 \pm 7.14 \times 10^5$ cells mL^{-1} ($n = 14$). The number of heterotrophic bacteria was significantly greater under thin snow throughout the spring (paired t test, $t_{15} = 2.396$, $p = 0.031$), which was reflected by the higher average abundance of cells under thin snow at $2.8 \pm 2.8 \times 10^6$ cells mL^{-1}, than that under thick snow at $2.3 \pm 1.6 \times 10^6$ cells mL^{-1} ($n = 15$).

Fig. 3

a Abundance of heterotrophic bacteria (cells × 10^6 mL^{-1}) measured with flow cytometry (*bars*) under thin (*dark gray*) and thick (*light gray*) snow covers. Bacterial production (*dots*) with the standard deviation between replicates (n = 2) over the sampling period is also shown for cells under thin (*solid*) and thick (*open*) snow covers. **b** Daily bacterial production normalized by bacterial abundance in sea ice under thin (*solid*) and thick (*open*) snow covers

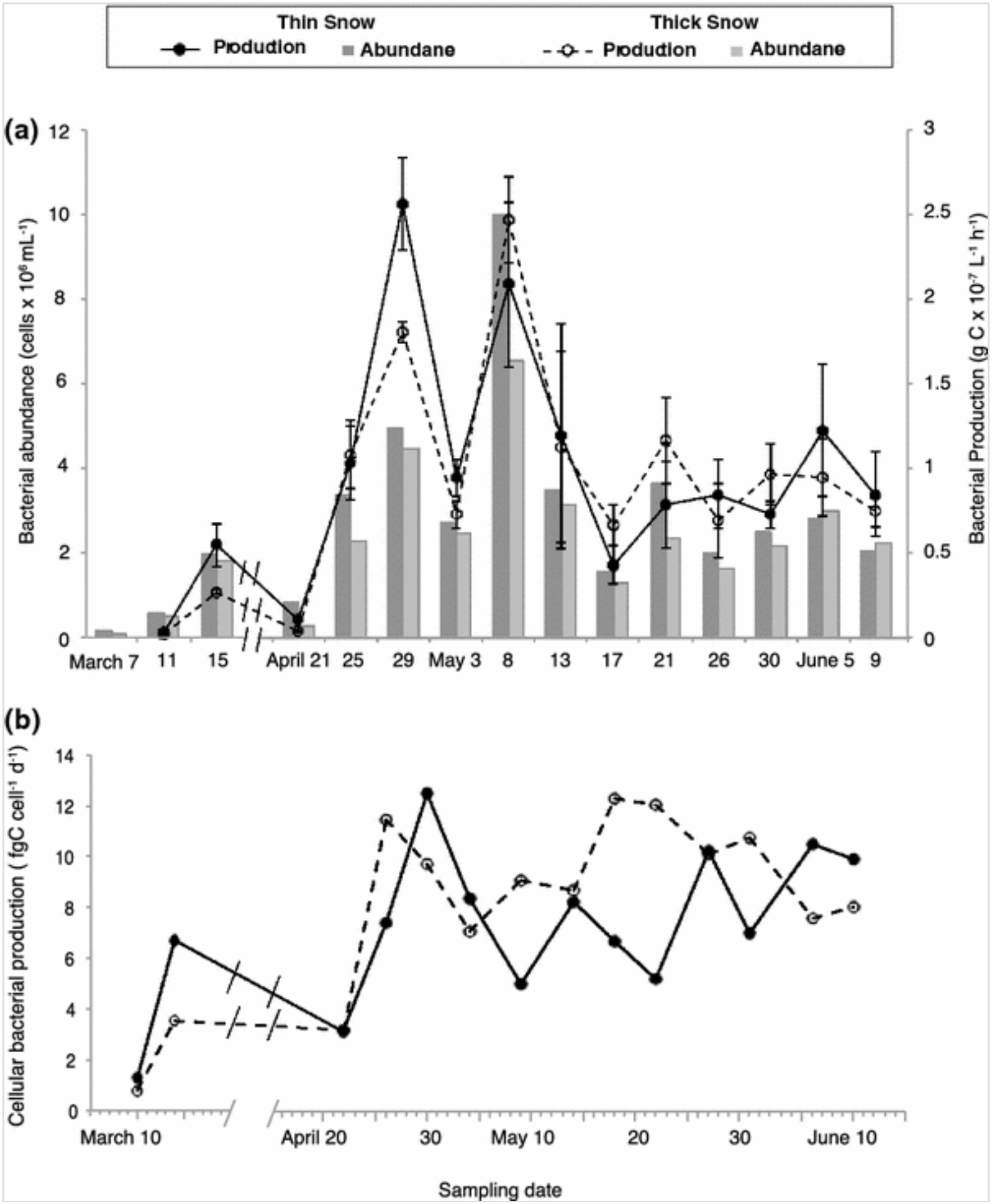

Bacterial production and heterotrophic bacterial abundance were strongly correlated under thin ($r = 0.836$, $p = 0.0002$, $n = 14$) and thick ($r = 0.940$, $p < 0.0001$, $n = 14$) snow covers, and seasonal trends in production were similar to those described above for cell abundance (Fig. 3a). Production peaked between 29 April and 8 May at 3.8×10^{-7} g C L^{-1} h^{-1} under thin snow and 4.1×10^{-7} g C L^{-1} h^{-1} under thick snow. After 8 May, production was relatively constant averaging $1.5 \times 10^{-7} \pm 3.9 \times 10^{-8}$ g C L^{-1} h^{-1} ($n = 14$) over the remaining study period. Overall, the rates of bacterial production were not statistically different between the snow covers (paired t test, $t_{14} = 0.480$, $p = 0.639$), and seasonal averages were similar at $1.6 \pm 1.1 \times 10^{-7}$ g C L^{-1} h^{-1} under thin snow and $1.5 \pm 1.1 \times 10^{-7}$ g C L^{-1} h^{-1} under thick snow ($n = 14$). Daily bacterial production normalized by bacterial abundance was generally <0.6 fgC $cell^{-1}$ d^{-1} until 25 April (Fig. 3b). It then increased to values in the range of 0.8–2.1 fgC $cell^{-1}$ d^{-1}, with no defined temporal trend and values that were not significantly different between thin and thick snow sites (paired t test, $t_{14} = -1.000$, $p = 0.336$,). Assuming a carbon content of 10 fgC $cell^{-1}$ d^{-1} (Ducklow 2000), this daily bacterial production equates to approximately 1 bacterium produced every 10 days for bacterial cells already present in the ice.

Abundance of cyanobacteria and eukaryotes in sea ice

The abundance of cyanobacteria was low throughout the spring, and on several occasions cyanobacteria were not documented in the samples analyzed (Fig. 4). Cyanobacterial counts in the bottom ice remained below 171 cells mL^{-1} under thin snow, with the exception of a perceived outlier on 8 May where the concentrations reached nearly 550 cells mL^{-1}. They did not exceed 138 cells mL^{-1} under thick snow throughout the study. There was no significant difference in the abundance of cyanobacteria between thin and thick snow (paired t test, $t_{15} = 1.362$, $p = 0.195$).

Fig. 4

Flow cytometry measurements of picoeukaryote (*light gray*), nanoeukaryote (*dark gray*), and cyanobacteria (*black*) abundance under thin (**a**) and thick (**b**) snow covers

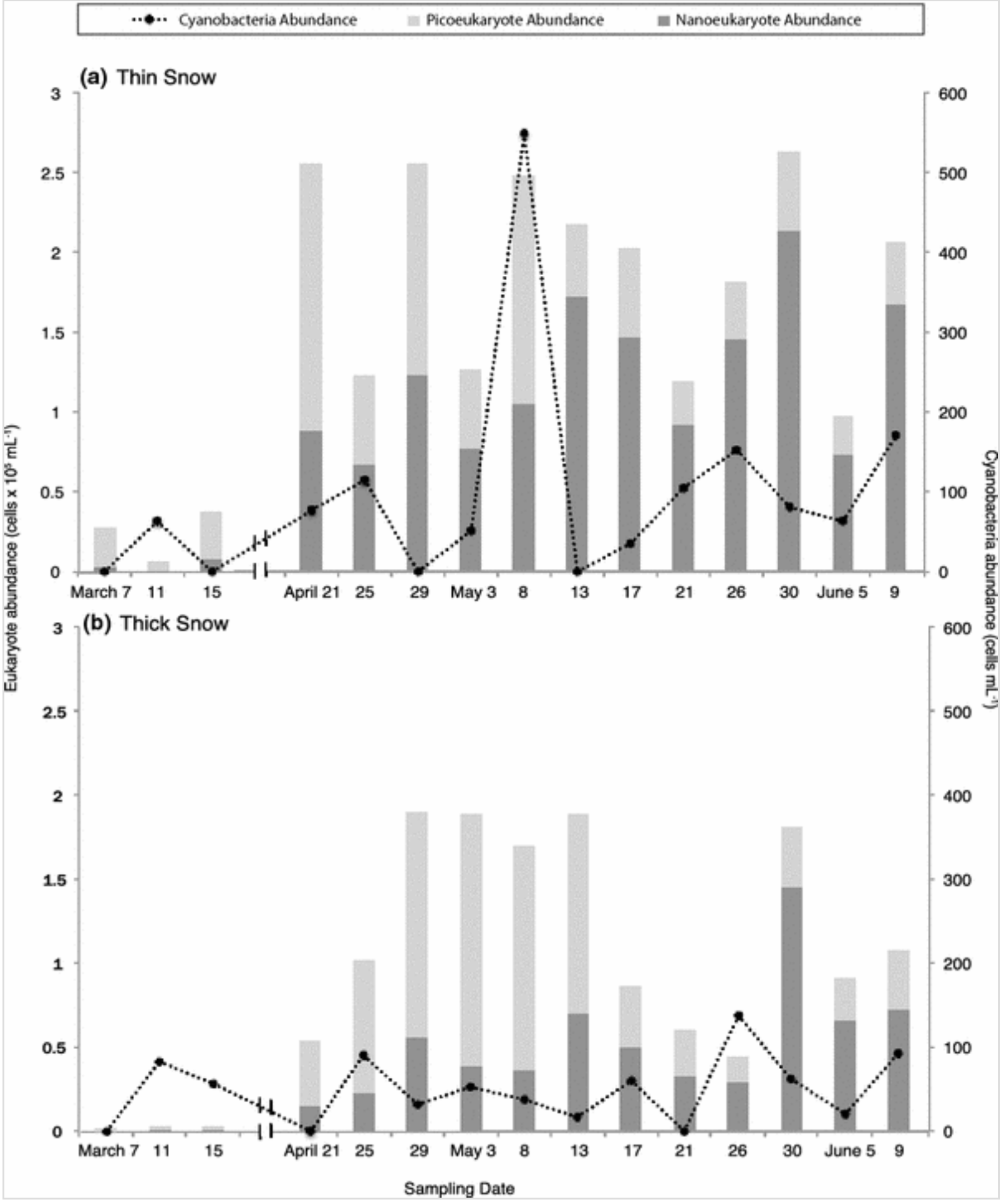

The abundance of photosynthetic picoeukaryotes over the spring is shown in Fig. 4, where the concentration of cells in the bottom ice was lowest in March and highest between 21 April and 30 May. Relative to the total abundance of algae in the ice, percent abundance of picoeukaryotes decreased under thin snow from 87% (2.5×10^4 cells mL^{-1}) to 11% (3.8×10^4 cells mL^{-1}) over the sampling period ($r = -0.929$, $p < 0.0001$, $n = 14$) (Fig. 5). Similarly, the relative abundance of picoeukaryotes under thick snow decreased from 73% (1.1×10^3 cells mL^{-1}) to 19% (3.5×10^4 cells mL^{-1}) over the spring ($r = -0.823$, $p = 0.0002$, $n = 15$). The

numerical abundance of picoeukaryotes was not significantly different between snow depths (paired *t* test, $t_{14} = 0.259$, $p = 0.799$) although the relative abundance of picoeukaryotes was significantly lower under thin than thick snow (paired *t* test, $t_{15} = -2.741$, $p = 0.016$), with an average of 35 ± 28% ($5.9 \pm 4.8 \times 10^4$ cells mL^{-1}) versus 43 ± 26% ($5.5 \pm 5.3 \times 10^4$ cells mL^{-1}) ($n = 15$), respectively (Fig. 5).

Fig. 5

Percent abundance of picoeukaryote (<2 μm, *light gray*) and average nanoeukaryote (2–20 μm, *dark gray*) and microeukaryote (21–200 μm, *black*) cells in the bottom ice at the beginning (7 March), middle (8 May), and end (9 June) of the spring. The average size composition of the sea ice algal community for the entire sampling period is also presented

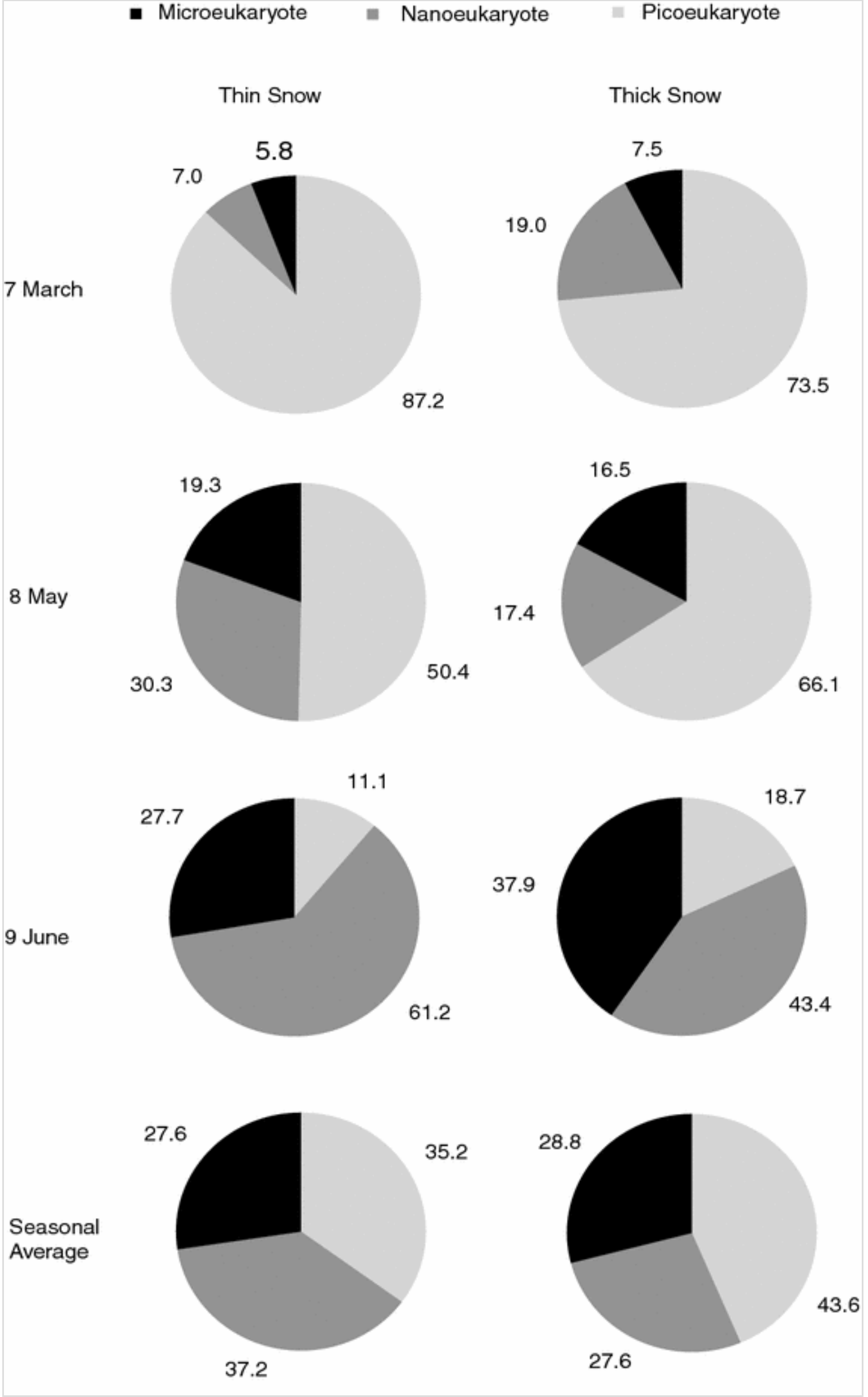
Microeukaryote
Nanoeukaryote
Picoeukaryote
Thin Snow
Thick Snow
7 March
5.8
7.0
87.2
7.5
19.0
73.5
8 May
19.3
30.3
50.4
16.5
17.4
66.1
9 June
11.1
27.7
61.2
18.7
37.9
43.4
Seasonal Average
27.6
35.2
37.2
28.8
43.6
27.6

Cell abundance of photosynthetic nanoeukaryotes measured with the flow cytometer (Fig. 4) was significantly higher under thin than thick snow covers (paired *t* test, $t_{15} = 5.629$, $p < 0.0001$). The seasonal increase in cell abundance was also greater under thin ($r = 0.795$, $p = 0.0004$, $n = 15$) than thick ($r = 0.719$, $p = 0.003$, $n = 15$) snow cover. Similarly, nanoeukaryote abundance estimated from light microscopy showed an increase over time (Fig. 6) under thin snow ($r = 0.806$, $p = 0.002$, $n = 15$) and thick snow ($r = 0.582$, $p = 0.023$, $n = 15$), and the number of estimated nanoeukaryotes was greatest under thin snow cover (paired *t* test, $t_{15} = -2.659$, $p = 0.019$, $n = 15$). Relative cell abundance of all nanoeukaryotes (results from flow cytometry and light microscopy were averaged for each sample) increased over the spring from 7 to 61% under thin snow ($r = 0.855$, $p < 0.0001$, $n = 15$) and from 19 to 43% under thick snow ($r = 0.683$, $p = 0.005$, $n = 15$) (Fig. 5).

Fig. 6

Cell abundance time series of nanoeukaryotes (2–20 μm, *light gray*) and microeukaryotes (21–200 μm, *dark gray*) under thin (**a**) and thick (**b**) snow covers, enumerated over the spring using inverted light microscopy. Seasonal change in estimated daily production from Campbell et al. (2016) is also shown (*line*)

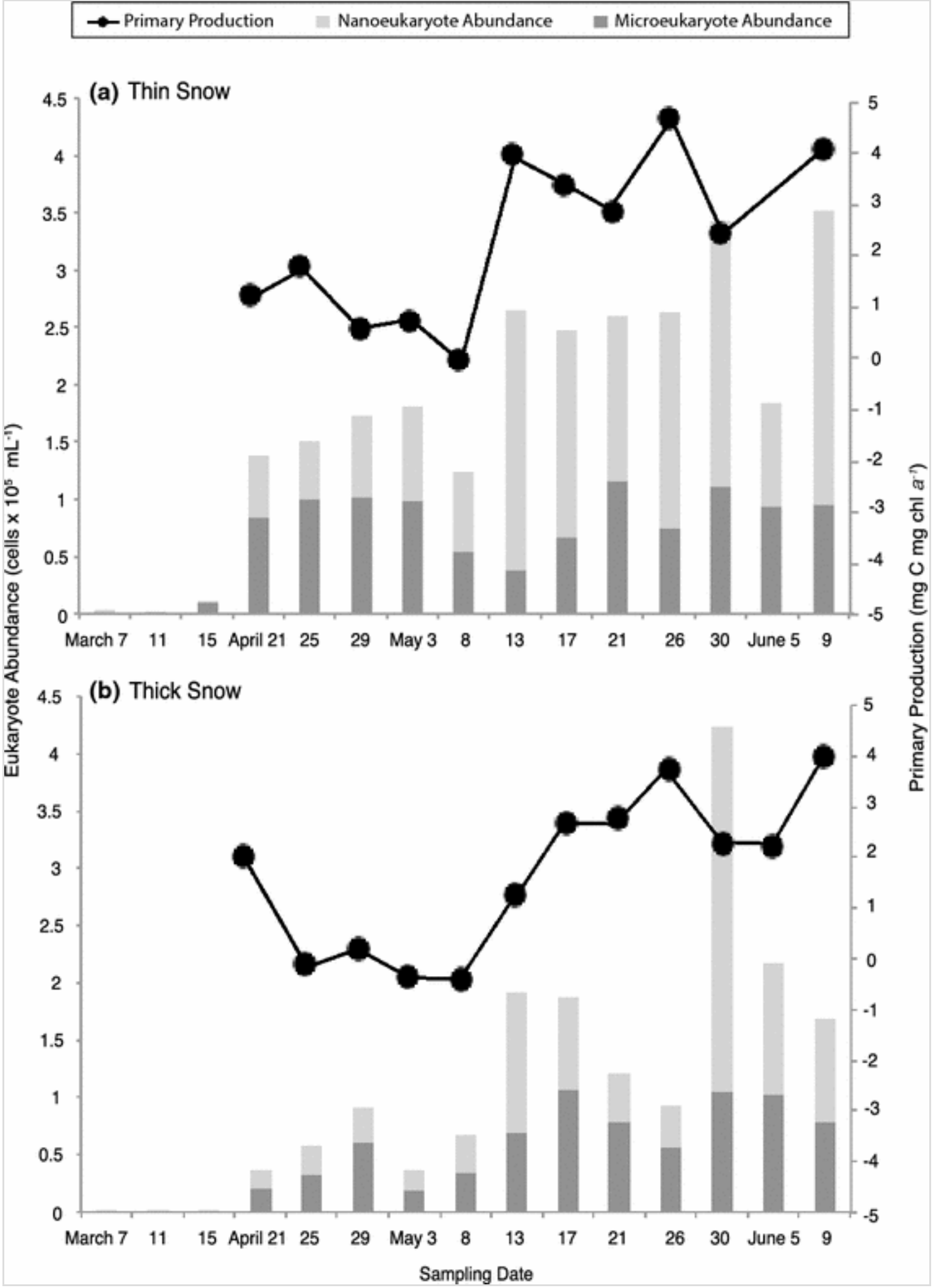

Microeukaryotes were significantly more abundant under thin snow cover (paired *t* test, $t_{15} = 2.316$, $p = 0.036$), averaging $7 \pm 3.8 \times 10^4$ versus $5 \pm 3.8 \times 10^4$ cells mL^{-1} ($n = 15$). The relative abundance of microeukaryotes showed a similar trend to nanoeukaryotic cells over the spring, and increased from 6 to 28% ($r = 0.589$, $p = 0.021$, $n = 15$) under thin snow and from 8 to 38% ($r = 0.743$, $p = 0.002$, $n = 15$)

under thick snow (Fig. 5).

Total algal abundance and production

The total number of ice algal cells counted with light microscopy increased in thin ($r = 0.895$, $p < 0.0001$, $n = 15$) and thick ($r = 0.718$, $p = 0.003$, $n = 15$) snow-covered sea ice over spring and was significantly higher under thin snow cover (paired t test, $t_{15} = 3.428$, $p = 0.004$). This was also true for the calculated daily average production of algae collected from thin ($r = 0.693$, $p = 0.018$, $n = 11$) or thick ($r = 0.648$, $p = 0.023$, $n = 12$) snow over time, which was significantly greater (paired t test, $t_{11} = 2.454$, $p = 0.034$, $n = 11$) under thin snow at 1.7 ± 1.4 mg C mg chl a^{-1} ($n = 11$) than under thick snow cover at 1.1 ± 1.4 mg C mg chl a^{-1} ($n = 12$) (Fig. 6).

Taxonomic composition of the ice algal community

A total of 63 species were identified and counted in the bottom ice over our sampling period (Online Resources 3, 4). The protist group with the most cells enumerated for thin and thick snow-covered sea ice was large (5–15 μm) and solitary *Attheya* spp., followed by small (5 μm) *Attheya* spp. that were primarily found attached to the third most abundant taxa, *N. frigida*. The small and largely epiphytic fraction of *Attheya* spp. comprised 29.4 ± 11.7% of cells in the genus *Attheya* (inclusive of *Attheya longicornis* and *Attheya septentrionalis*) under thin snow and 43.2 ± 14.1% under thick snow ($n = 15$). Pennate diatoms *Navicula pelagica* (average 5966 ± 6125 cells mL^{-1}, $n = 15$) and *Pseudo-nitzschia delicatissima* (average 2378 ± 2540 cells mL^{-1}, $n = 15$) were also abundant in the samples analyzed (Online Resources 3, 4).

The relative abundance of the main protist groups collected from sea ice under thin and thick covers is presented in Fig. 7 (see Online Resources 3 and 4 for detailed taxonomic information and cell counts). Diatoms were the dominant group throughout the spring, consistently accounting for over 60% of the eukaryotes enumerated using light microscopy. However, whether pennate or centric diatoms were most abundant in the bottom ice was dependent on the sampling date and the depth of snow cover.

Fig. 7

Percent composition of the main protist groups in the bottom ice under thin (**a**) and thick (**b**) snow covers. Seasonal changes in pennate (*open circle*) and centric (*solid circle*) diatom abundance are also highlighted. *Dashed lines* indicate the average

pennate and centric diatom abundance in sea ice of the Canadian Arctic (see Poulin et al. 2011)

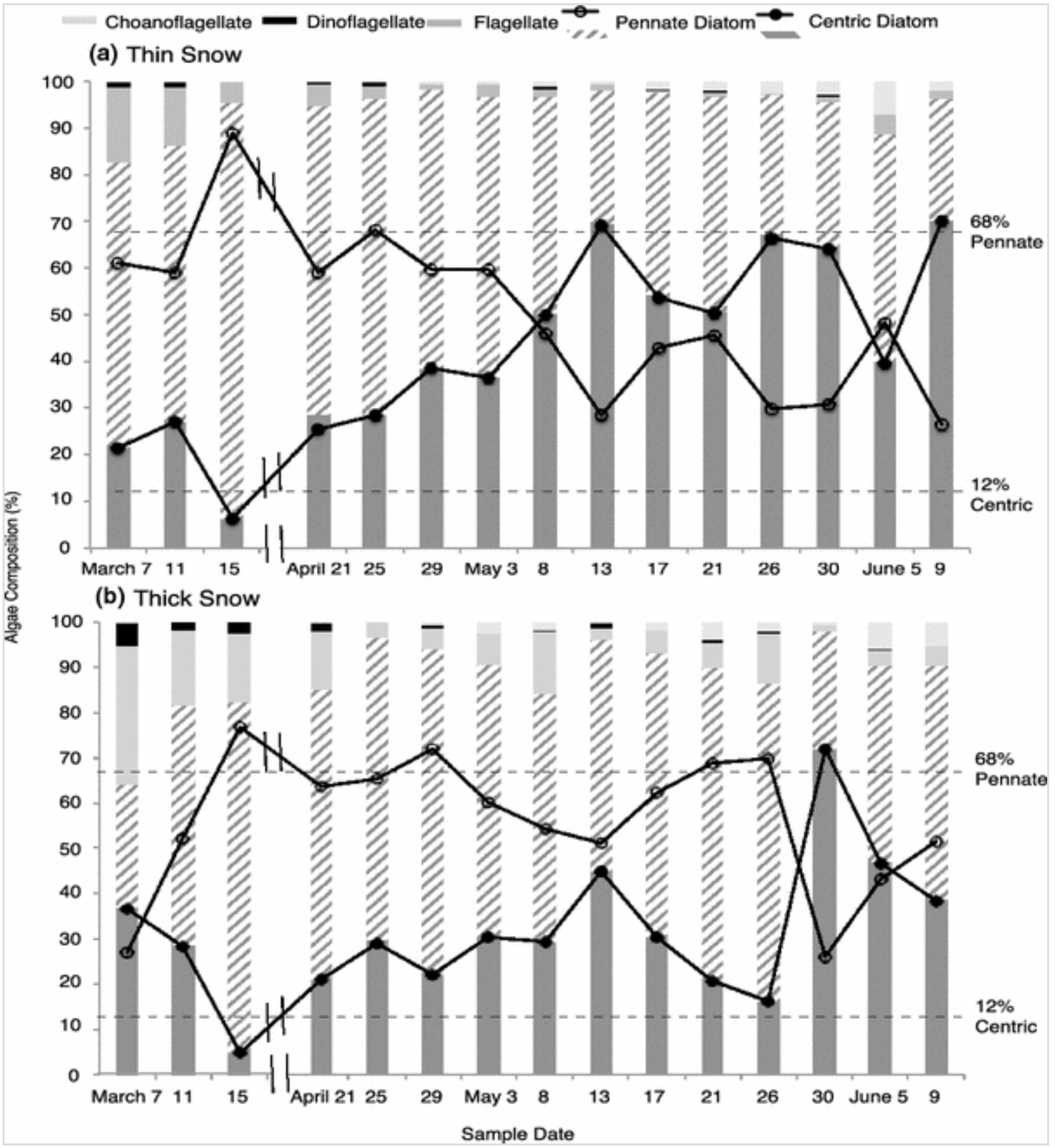

The number of both centric ($r = 0.792$, $p = 0.0004$, $n = 15$) and pennate ($r = 0.800$, $p = 0.0003$, $n = 15$) diatoms increased over the spring under thin snow (Online Resource 3). However, the percent abundance of centric diatoms increased significantly ($r = 0.795$, $p = 0.0004$, $n = 15$) as the percent abundance of pennate diatoms decreased ($r = -0.738$, $p = 0.002$, $n = 15$) (Fig. 7a). The shift in dominance between these protist groups occurred on 8 May, where the abundance of centric diatoms remained largely above 50% and pennate diatoms remained below 50% after

this date. Centric diatoms under thin snow represented 43.5 ± 19.1% of the bottom-ice community on average, while pennate diatoms accounted for 50.5 ± 17.5% (n = 15).

The number (r = 0.513, p = 0.05, n = 15) and percent abundance (r = 0.429, p = 0.110, n = *15*) of centric diatoms did not change significantly over the spring under thick snow, with an average abundance of 4.9 ± 7.8 × 10^4 cells mL^{-1} (n = 15). In comparison, a seasonal increase in the number of pennate diatoms (r = 0.849, $p < 0.0001$, n = 15) was observed from 114 to 8.7 × 10^4 cells mL^{-1} (Online Resource 4). However, this increase in pennate diatoms was not enough to influence a significant trend in relative abundance of pennate diatoms over the spring (r = −0.044, p = 0.877, n = 15) (Fig. 7b). Pennate diatoms dominated the bottom-ice community under thick snow for the majority of the sampling period, comprising 56.1 ± 15.1% of cells on average, while centric diatoms accounted for 31.5 ± 15.5% (n = 15). The number of centric and pennate diatoms was greater under thin than thick snow (paired t test, t_{15} = 2.625, p = 0.020; paired t test, t_{15} = 2.414, p = 0.03, respectively), but centric diatoms accounted for a larger fraction of the bottom-ice community under thin snow cover (paired t test, t_{15} = 2.575, p = 0.022) (Fig. 7).

After diatoms, flagellates were the next most abundant protist group, ranging between 1.2 (29 April) and 16.3% (7 March) of cells under thin snow, and 1.4 (30 May) and 30.9% (7 March) under thick snow (Online Resources 3, 4) (Fig. 7). The number of flagellates increased over the season (Online Resources 3, 4), but their overall relative abundance in the bottom-ice community declined significantly under thin and thick snow (Fig. 7), with the linear correlation coefficients of −0.730 (p = 0.002, n = 15) and −0.797 (p = 0.0003, n = *15*), respectively. Flagellate abundance was not significantly different between snow depths (paired t test, t_{15} = −1.301, p = 0.214), but their percent contribution to the community was greatest under thick snow cover (paired t test, t_{15} = −4.366, p = 0.001) (Fig. 7).

The number of choanoflagellates identified in the ice was <12.6 × 10^3 cells mL^{-1} (Online Resources 3, 4), and accounted for <7% of the ice community under thin snow and <6% under thick snow (Fig. 7). Their numerical abundance which was not significantly different between snow depths (paired t test, t_{15} = 1.568, p = 0.139) increased over the spring under both thin (r = 0.780, p = 0.001, n = 15) and thick (r = 0.698, p = 0.004, n = 15) snow. The abundance of dinoflagellates in the bottom ice was also low at <1.1% (<1.3 × 10^3 cells mL^{-1} This should be on the same line as mL) and <5% (<1.7 × 10^3 cells mL^{-1}) under thin and thick snow covers, respectively (Online

Resources 3, 4) (Fig. 7). Dinoflagellate abundance was not different between snow covers (paired *t* test, $t_{15} = -0.301$, $p = 0.768$) and did not exhibit any seasonal trends. Ciliates were often not documented in the ice and also showed no significant trends in absolute or relative abundance.

Controls of bacterial abundance and production

Pearson correlation coefficients were calculated for heterotrophic bacterial abundance and production versus sea ice chl *a*, E_Z(PAR), bottom-ice temperature, and bulk salinity under thin snow, interface DOC, and the abundance of picoeukaryotes, nanoeukaryotes, and choanoflagellates (data not shown). Significant correlations ($p < 0.05$) between bacterial abundance and production were only observed for picoeukaryote abundance, after an apparent outlier on 21 April was removed (Fig. 8). The number of cyanobacteria under thin snow increased with the abundance of heterotrophic bacteria ($r = 0.766$, $p = 0.001$, $n = 15$). However, cyanobacteria were not correlated with any of the parameters listed in Online Resource 2 under thick snow cover (data not shown).

Fig. 8

Linear regressions between heterotrophic bacterial abundance (**a**) and bacterial production (**b**) with prokaryotic algal cell abundance, independent of an outlier on 21 April (*circle*). Samples were collected from under thin (*black, solid line*) or thick (*gray, dashed line*) snow covers. Significant ($p < 0.05$) linear models of the data are also shown

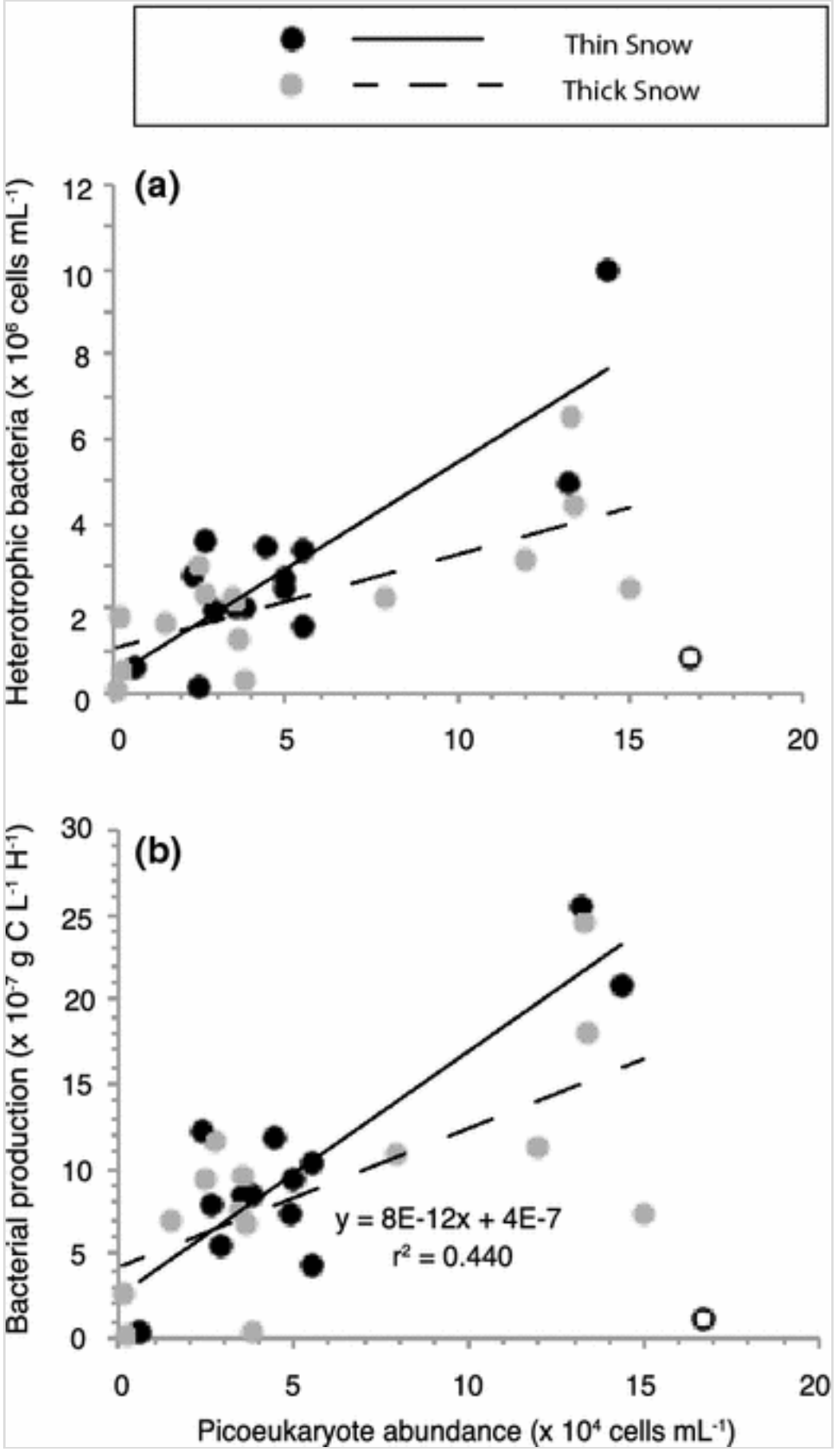

Controls on ice algal community composition

Linear correlations between sea ice environmental parameters and size classes of algae are summarized in Online Resources 5 and 6 for thin and thick snow covers, respectively. Picoeukaryote abundance was not correlated with any of the environmental parameters assessed. However, nanoeukaryote abundance measured using the flow cytometer, estimated from light microscopy, or the average from the two methods increased with E_z(PAR) under thin or thick snow-covered sea ice, respectively (Online Resources 5, 6). Nanoeukaryote abundance under thin snow cover also decreased with the concentration of ice NO_x (Online Resource 5), while

microeukaryote abundance increased with E_z(PAR) under thick snow (Online Resource 6).

Linear correlations between sea ice environmental parameters and the presence of the three dominant protist groups (centric diatoms, pennate diatoms, and flagellates) under thin (Online Resource 7) and thick (Online Resource 8) snow were also investigated. Centric diatom abundance under thin and thick snow covers, and pennate abundance under thick snow increased significantly with E_z(PAR) (Online Resources 7, 8). However, the type of correlation (positive or negative) between centric or pennate diatoms and E_z(PAR) was opposite when considering their relative contribution to the bottom-ice community. No other significant correlations were documented for these diatoms under thick snow.

The abundance of choanoflagellates increased with centric diatom abundance ($r = 0.605$, $p = 0.017$, $n = 15$) under thin snow and pennate diatom abundance under thick snow ($r = 0.568$, $p = 0.027$, $n = 15$). Their abundance was also positively correlated with the intensity of E_z(PAR) under thin ($r = 0.780$, $p = 0.005$, $n = 11$) or thick ($r = 0.853$, $p = 0.001$, $n = 11$) snow. The abundance of heterotrophic flagellates decreased significantly with NO_x concentration in the ice under thin snow and showed an increase with all parameters except ice NO_x under thick snow (Online Resource 8). The percent abundance of flagellates decreased with E_z(PAR) under thick snow.

Controls of ice algal chlorophyll *a*, carbon, and production

The potential impact of cell size and/or taxonomic composition on chl *a*, POC, and estimated daily primary production was investigated through linear correlation analysis (Online Resources 5–8). Chlorophyll *a* and POC increased with nanoeukaryote and microeukaryote abundances, under thin and thick snow, but were not correlated with the concentration of picoeukaryotes (Online Resources 5, 6). Chlorophyll *a* and POC also increased significantly with the abundance of all protist groups, with the exception of flagellate abundance under thick snow (Online Resources 7, 8). However, the type of correlation (positive or negative) between chl *a*, POC, and percent abundance of the protist groups indicates that pigment and carbon abundance increased with the dominance of centric diatoms in the algal community and decreased with the proportion of pennate diatoms and/or flagellate cells.

Primary production decreased with picoeukaryote abundance under both snow

covers and was significantly correlated with nanoeukaryote abundance (derived from light microscopy and average abundance) under thin snow, where the relationship was positive (Online Resource 5). Production also increased with centric diatoms (abundance or percent composition) and decreased with the relative abundance of pennate diatoms under thin snow (Online Resource 7). Primary production was not significantly correlated with any of the protist groups under thick snow cover.

Discussion

Controls of heterotrophic bacterial abundance and production

The number of heterotrophic bacteria present in the sea ice was within the wide range of estimates that have been reported for spring or summer sea ice in the Arctic, from 5×10^5 (Maranger et al. 1994) to 16.4×10^{10} cells mL^{-1} (He et al. 2005). Bacterial production was also representative of literature values for Arctic sea ice, where production over the spring was within the range of 3.6×10^{-8} (Maranger et al. 1994) to 3.1×10^{-6} g C l^{-1} h^{-1} (Kaartokallio et al. 2013).

The strong relationships between bacterial abundance and production with the number of picoeukaryotic cells may be due to increased supply of labile dissolved carbon, as diffusive release of DOC is greater from picoeukaryotes than larger cells as a result of a higher surface area-to-volume ratio (López-Sandoval et al. 2011). This supply of organic substrate by ice algae is a well-documented control of bacterial production (e.g., Bunch and Harland 1990; Mock et al. 1997; Søgaard et al. 2013), but our results suggest that it is the smallest group of algae that could be most important to this relationship. Unfortunately, DOC concentrations from the bottom ice were not available to confirm this hypothesis, and thus further work on the contribution of sea ice picoeukaryotes to bacterial production and the microbial loop is merited. We note that seasonal increases in bacterial abundance and production could also be related to gravity-driven movement of brine previously isolated higher in the ice profile toward the ice bottom, as it would transport cells and additional organic carbon for production (Deming 2010). Such movement of brine is possible once the upper ice profile warms to −5 °C and reaches 5% porosity (Golden et al. 1998), which was observed during this study period as of 17 May under thin snow cover (Campbell et al. 2016).

The strong correlations between bacterial abundance and production (“Abundance of cyanobacteria and eukaryotes in sea ice” section) indicate that the majority of bacterial cells present in the ice were respiring. However, the increased bacterial

production per cell (Fig. 3b) after 25 April when bacterial abundance largely showed low seasonal variability (Fig. 3a) indicates that one or a combination of the following were important factors: increasing productivity per cell over the spring, cell loss via grazing, and cell death following virus-induced lysis. Unfortunately, we do not have sufficient data to evaluate the specific contribution of each potential factor here.

AQ2

Using flow cytometry and light microscopy to estimate nanoeukaryote abundance

The abundance of nanoeukaryotes counted with the flow cytometer versus enumerated from light microscopy is shown in Fig. 9. The comparison shows that flow cytometry provided slightly higher estimates of cell counts (i.e., above the 1–1 line) at or below microscopy-derived cell concentrations of approximately 0.8×10^5 cells mL^{-1}, but lower counts (i.e., below the 1–1 line) above this threshold, relative to light microscopy. Higher flow cytometry-based counts of nanoeukaryotes at low cell densities likely represent the effectiveness of the flow cytometer in counting small cells that are easily missed when using a light microscope (Tremblay et al. 2009), while overestimates of cell abundance from light microscopy have been attributed to the Lugol's staining process that can introduce difficulty in distinguishing cells and separating autotrophic from heterotrophic cells (Sherr and Sherr 1993; Tremblay et al. 2009).

Fig. 9

Abundance of estimated nanoeukaryotic cells using light microscopy, versus nanoeukaryotic cell counts from FC analysis of samples under thin (*black*) and thick (*gray*) snow covers. Power functions (*solid*) and a 1–1 line (*dashed*) are also presented

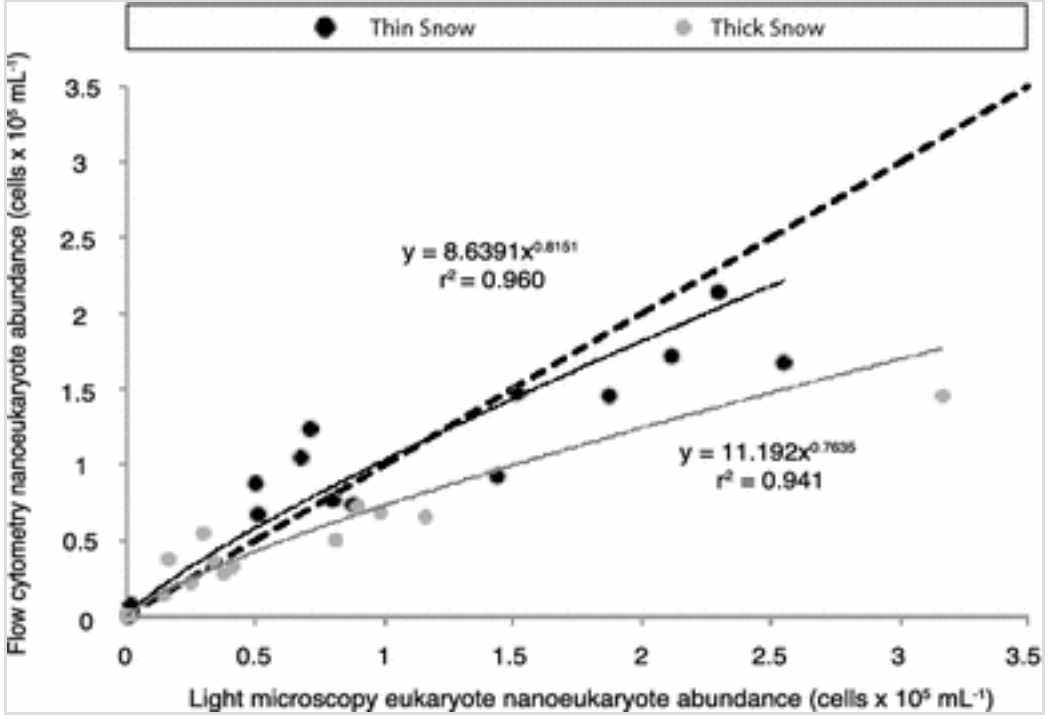

Data of light microscope versus flow cytometer-based cell counts in Fig. 9 deviated from the ideal 1–1 relationship to a greater extent under thick snow. This deviation could partially be a result of one data point under thick snow with especially high cell counts following light microscopy analysis. It may also highlight that the difference in nanoeukaryote abundance between methods was greatest under thick snow cover due to taxonomic differences. Nanoeukaryotic algae under both snow covers were dominated by centric diatoms (Online Resources 3, 4), which comprised 80.7 ± 17.5% of nanoeukaryotes under thin snow and 63.8 ± 19.1% under thick snow (n = 15). However, the relative abundance of pennate diatoms <20 µm was greater under thick snow at 13.2 ± 7.4% in comparison to 8.9 ± 7.1% under thin snow (n = 15). We suggest that the flow cytometer may not have been able to ~~*record*~~ record pennate diatoms as effectively as centric diatoms because the apical axis of pennates was often estimated to be close to 20 µm, the maximum size detected by the flow cytometer (Online Resources 3, 4). Our classification of nanoeukaryotes from light microscopy likely compounded this error, as cells deemed <20 µm based on literature size estimates could have been slightly larger. In comparison, centric diatoms that were predominantly of the genus *Attheya* (Online Resources 3, 4) had apical and pervalvar axes well within the nanoeukaryotic range. Finally, the proportion of *Attheya* spp. that was epiphytic was greater under thick snow (see "Taxonomic composition of the ice algal community"). These cells living largely in association with *N. frigida* may not have been counted separately by the flow cytometer, which would have contributed to a perceived underestimate of cell abundance relative to estimates from light microscopy. As a result, we conclude that flow cytometry is an effective tool at efficiently measuring the abundance of pico- and nanoeukaryotes in sea ice. However, caution is advised when measuring the abundance of cells whose sizes are close to the detection limit. In these instances,

and for measuring microeukaryote abundance, light microscopy remains the favored approach.

Seasonal controls of algal cell size

The concentration of picoeukaryotes in this study was within the range reported for sea ice by Piwosz et al. (2013), except for the peaks in abundance observed between 29 April and 13 May that reached nearly 1.5×10^5 cells mL^{-1} (Fig. 4). These peaks roughly corresponded to the increases observed in the number of heterotrophic bacteria (Fig. 3), where the presence of picoeukaryotes is thought to have positively affected the number of heterotrophic bacteria and their production in the ice by providing DOC. The high peaks in picoeukaryote abundance could also have been aided by the tolerance of picoeukaryotes for nutrient-limited environments (Agawin et al. 2000), like the nitrogen conditions (average 0.74 ± 0.49 μmol L^{-1}, $n = 30$) described for sea ice in the study region (Campbell et al. 2016). Despite the relatively high abundance of picoeukaryotes in this study, we note that they did not significantly correlate with chl *a*, POC, or primary productivity (Online Resources 2, 3). Using the cellular quota of 0.025 pg chl *a* $cell^{-1}$ proposed by Tremblay et al. (2009), picoeukaryotes contributed $1.2 \pm 1.1\%$ of chl *a* under thin snow and $2 \pm 1.2\%$ under thick snow ($n = 15$). These average estimates support a minimal contribution of picoeukaryotes to chl *a,* or alternatively could indicate that the picoeukaryotes in this study were mixotrophic to some extent.

Light availability is a well-documented control of chl *a* and particulate carbon during the accumulation phase of the ice algal bloom (e.g., Gosselin et al. 1985; Mundy et al. 2005; Różańska et al. 2009; Campbell et al. 2015). The significant positive correlations between nanoeukaryote algae and E_z(PAR) under both snow covers support the importance of light availability for algae 2–20 μm in this study. Furthermore, linear regression analyses performed on average nanoeukaryote abundance and all environmental parameters indicate that light was the dominant control (highest r^2, Online Resource 9), significantly accounting for 65% of variability in nanoeukaryote abundance under thin snow and 48% under thick snow. Light availability likely influenced microeukaryote abundance under thick snow, where correlations between the parameters were significant (Online Resource 6) and E_Z(PAR) significantly accounted for 63% of variability in microeukaryote abundance (Online Resource 10). The absence of a similar relationship under thin snow could potentially highlight that microeukaryotes present experienced less light limitation due to the higher light conditions (Fig. 2).

Significant correlations between chl *a*, POC, and nanoeukaryotes or microeukaryotes suggest that algae >2 μm drove changes in chl *a* and POC (Online Resources 5, 6). This is perhaps not surprising given that the majority of nanoeukaryotes and microeukaryotes in this study were diatoms (Online Resources 3, 4), which can replicate quickly in response to the favorable light conditions in the Arctic spring (Miller and Wheeler 2012). These findings also support previous observations that showed significant correlations between chl *a* and nanoeukaryote abundance in sea ice (Comeau et al. 2013), and cells >5 μm accounting for 50–100% of ice algal biomass (Gosselin et al. 1997). Further calculation of linear regressions indicates that the contribution of microeukaryotes to overall chl *a* and POC concentrations was either insignificant or less important (lower β) than nanoeukaryotes, with the exception of chl *a* under thick snow (see Online Resource 11).

Picoeukaryote abundance in sea ice can also be controlled by light availability and has been negatively correlated with snow thickness as a result of its attenuation properties (Piwosz et al. 2013). Significant relationships between the number of picoeukaryotes and PAR were not specifically documented in this study (Online Resources 5, 6); however, picoeukaryote abundance was significantly greater under the higher light conditions of thin snow cover (see "Abundance of cyanobacteria and eukaryotes in sea ice").

The seasonal shift in the percent composition of the ice algal community from the dominance of small to large cells was associated with the percent increase of nanoeukaryotes under thin snow, and similar increases of nanoeukaryotes and microeukaryotes under thick snow (Fig. 5). Increasing primary production over the spring that was driven by increasing PAR transmission through the ice (Campbell et al. 2016) was mostly influenced by these increases in nano- and microeukaryotes (Figs. 4, 6). The strength of linear regressions further suggests that nanoeukaryotes largely controlled production under thin snow ($r^2 = 0.546$, $p = 0.009$, $n = 11$), while microeukaryotes were perhaps slightly more important under thick snow cover ($r^2 = 0.256$, $p = 0.093$, $n = 12$) (see Online Resource 11). These observations support conclusions by Gosselin et al. (1997) that algae >5 μm account for the majority of production in Arctic sea ice, despite the high potential of picoeukaryotes to contribute to primary production as a result of their high growth rates (Agawin et al. 2000).

Seasonal controls of ice algal taxonomic composition

Diatoms typically dominate the bottom-ice algal assemblage, with pennate diatoms comprising 68% and centric diatoms 12% of average communities in the Canadian Arctic (Poulin et al. 2011). In comparison to these averages, the proportion of pennate diatoms was low and that of centric diatoms was high in our study (Fig. 7), particularly under thin snow cover where centric species of the genus *Attheya* were abundant (Online Resource 3). Centric diatoms like *A. septentrionalis*, in addition to *Melosira arctica* (not documented here), are commonly found in Arctic sea ice (Riedel et al. 2003; Różańska et al. 2008, 2009; vonQuillfedt et al. 2009; Poulin et al. 2011). However, it is the cryophilic pennate diatom *N. frigida* that is considered to be the sentinel species of this environment (Poulin et al. 2011; Leu et al. 2015). We surmise that species of *Attheya* may have been able to outcompete *N. frigida* in our study area of Dease Strait due to the relatively fresh surface waters and nitrogen-limited conditions (see "Study site and environmental conditions") (Campbell et al. 2016), as centric diatoms likely have a greater tolerance for low-salinity and low-nitrogen environments (Melnikov et al. 2002). The surface area-to-volume ratio of the small *Attheya* spp. is also slightly greater than the comparatively large cells of *N. frigida*. This size difference leads to a greater nutrient uptake potential per growth requirement (Miller and Wheeler 2012) for *Attheya* spp. that could allow them to outcompete larger diatoms for nutrients. However, negative correlations between the numerical abundance of all ($n = 30$) *Attheya spp.* (r_{ice} −0.549, $p = 0.002$; $r_{water} = -0.384$, $p = 0.036$) or *N. frigida* ($r_{ice} = -0.419$, $p = 0.021$; $r_{water} = -0.415$, $p = 0.023$) and NO_x (bulk ice or interface) indicate that both species tolerated increasing nitrogen limitation. We note that correlations between the numerical abundance of all ($n = 30$) *Attheya spp.* ($r = 0.525$, $p = 0.003$) or *N. frigida* ($r = 0.447$, $p = 0.013$) and interface salinity were inconclusive.

Seasonal trends in diatom abundance under thin and thick snow covers (Fig. 7) appear to differ as a result of a rapid increase in *Attheya* spp. under thin snow (Online Resource 3). Although we suggest that the low surface water salinity and limited nutrients in the region facilitated the dominance of the centric diatom *Attheya spp*., the difference in absolute and relative abundances of this genus between thin and thick snow covers indicates that spatial variability across the study area was also important. We suggest that the higher light conditions characteristic of a thin snow cover (Fig. 2a) permitted centric diatoms to outcompete pennate diatoms at thin snow sites and resulted in the strong positive correlations observed between E_Z(PAR) and centric abundance (Online Resource 7). This is supported by previous observations that centric diatoms can be more numerous in thin sea ice as a result of greater light availability (Medlin and Priddle 1990; Melnikov et al. 2002).

Furthermore, it supports the conclusions by Różańska et al. (2009) that *A. septentrionalis* was more abundant in thin (<10 cm) than thick (>10 cm) snow-covered sea ice of the nearby Beaufort Sea as a result of differences in light availability.

The low relative abundance of other remaining protist groups is expected given the dominance of diatoms in this study (Fig. 6). For example, species of flagellates that typically account for approximately 6% of eukaryotes in sea ice of the Canadian Arctic (Poulin et al. 2011) represented about 4% of the algal population under thin snow and 10% under thick snow. Flagellate species are capable of dominating algal communities under low light conditions (Mikkelsen et al. 2008), and this likely explains the higher proportion of flagellates observed at the beginning of the spring and under thick snow cover (Fig. 7). Furthermore, limited or nil contributions of choanoflagellates (Poulin et al. 2011), cyanobacteria (Bowman et al. 2015), and ciliates (Riedel et al. 2007) to microbial communities in sea ice during the spring are known to occur.

The majority of nanoeukaryotes in this study were centric diatoms, while the majority of microeukaryotes were pennate diatoms (Online Resources 3, 4). As a result, the significant role of these size classes of algae in driving chl *a* and POC, as well as potentially primary production discussed previously, also applies to the importance of the protist groups of centric and pennate diatoms. For example, nanoeukaryotes had the greatest correlations with chl *a,* POC, and production under thin snow (Online Resource 5), as did centric diatoms (Online Resource 7). The significant correlations between the number of flagellates and chl *a* or POC concentrations (Online Resources 7, 8) also show that despite flagellates representing a small fraction of the sea ice community (Fig. 7) they may be an important contributor to nanoeukaryotic abundance. We note that negative correlations between NO_x and all three protist groups under thin snow cover highlight the likely presence of nitrogen limitation. This supports observations by Campbell et al. (2016) of a stronger nitrogen limitation influence under thin snow as a result of greater productivity rates, and therefore nutrient demand, at these locations.

AQ3

Conclusions

Environmental factors influencing the composition of the microbial community in the bottom of sea ice and their impact on chl *a*, POC, and productivity were

investigated in this research. Our time series of measurements showed that the size distribution and species composition of protist assemblages in the bottom ice changed over the spring and differed between depths of snow cover as a result of light intensity. It was suggested that pre-existing conditions, including surface water salinity and nitrogen availability, can influence the prevalence of algal species in a particular region. Such variability in microbial communities over time and space affects the concentration of chl *a,* POC, and potentially the primary productivity that is achieved. Future studies on species-specific responses to growth conditions would benefit this research, particularly for the species that are most often documented living in the bottom ice.

The most important algal group driving the spring bloom in this study was diatoms of the nano- and microeukaryotic size classes. The abundance of nanoeukaryotes, in particular, may be effectively analyzed using either flow cytometry or light microscopy; however, interpretation of flow cytometry measurements is cautioned when cells approach 20 μm in length. Picoeukaryotes were prominent members of the sea ice community during early spring, but they did not appear to influence chl *a,* POC, or production in the ice. Nevertheless, these algae remain an important aspect of the community through their anticipated link to heterotrophic bacteria and the sea ice microbial loop.

A likely fallout of climate warming is the reduction of nutrient inventories in many parts of the Arctic Ocean's surface waters (Tremblay et al. 2016). Studies have suggested that the reduction in nutrient inventories may favor small, picoeukaryotic cells, in the pelagic system (Tremblay et al. 2009; Li et al. 2009) because of their known affinity for low-nutrient conditions elsewhere in the global oceans (Legendre et al. 1987; Agawin et al. 2000). Our results indicate that the response of the sea ice algal community ~~unlikely~~does not likely result~~s~~ in picoeukaryote dominance, although the diatom community during the spring bloom may shift away from the typically dominant pennate diatom *N. frigida* toward centric forms like *Attheya* spp. Such changes are likely to have implications for the nutritional quality of grazer resources because of differences in fat content (e.g., Pogorzelec et al. 2017) and could affect the role sea ice algae play in sequestering carbon to the deep ocean if the sinking rates of species are found to differ substantially.

Acknowledgements

Support for this research was provided by a Northern Scientific Training Program grant and Natural Sciences and Engineering Research Council of Canada (NSERC)

Canadian Graduate Scholarship to KC, Canada Foundation for Innovation (CFI) and the Canada Excellence Research Chair grant to SR, NSERC Discovery and Northern Research Supplement Grants to CJM, and in-kind support from the Canadian High Arctic Research Station (CHARS). We thank Dr. Michel Gosselin and Ms. Sylvie Lessard for their support. This work represents a contribution to the research programs of ArcticNet, MEOPAR, the Arctic Science Partnership (ASP), and the Canada Excellence Research Chair unit at the Centre for Earth Observation Science (CEOS) at the University of Manitoba.

Electronic supplementary material

Below is the link to the electronic supplementary material.

Online Resource 1 (DOCX 46 kb)

Online Resource 2 (DOCX 46 kb)

Online Resource 3 (DOCX 85 kb)

Online Resource 4 (DOCX 85 kb)

Online Resource 5 (DOCX 50 kb)

Online Resource 6 (DOCX 48 kb)

Online Resource 7 (DOCX 48 kb)

Online Resource 8 (DOCX 48 kb)

Online Resource 9 (DOCX 47 kb)

Online Resource 10 (DOCX 46 kb)

Online Resource 11 (DOCX 51 kb)

References

Agawin NSR, Duarte CM, Agusti S (2000) Nutrient and temperature control of the contribution of picoplankton to phytoplankton biomass and production. Limnol Oceanogr 45:591–600

Belzile C, Brugel S, Nozais C, Gratton Y, Demers S (2008) Variations of the abundance and nucleic acid content of heterotrophic bacteria in Beaufort Shelf waters during winter and spring. J Mar Syst 74:946–956. doi:10.1016/j.jmarsys.2007.12.010

Bowman JS (2015) The relationship between sea ice bacterial community structure and biogeochemistry: a synthesis of current knowledge and known unknowns. Elementa 3:1–20. doi:10.12952/journal.elementa.000072

Bunch JN, Harland RC (1990) Bacterial production in the bottom surface of sea ice in the Canadian subarctic. Can J Fish Aquat Sci 43:1986–1995. doi:10.1139/f90-223

Campbell K, Mundy CJ, Barber DG, Gosselin M (2015) Characterizing the sea ice algae chl *a*-snow depth relationship over Arctic spring melt using transmitted irradiance. J Mar Syst 127:76–84. doi:10.1016/j.jmarsys.2014.01.008

Campbell K, Mundy CJ, Landy JC, Delaforge A, Michel C, Rysgaard S (2016) Community dynamics of bottom-ice algae in Dease Strait of the Canadian Arctic. Progr Oceanogr 149:27–39. doi:10.1016/j.pocean.2016.10.005

Caron DA, Gast RJ (2010) Heterotrophic protists associated with sea ice. In: Thomas DN, Dieckmann GS (eds) Sea ice, 2nd edn. Wiley Blackwell Publishing, Malaysia, pp 327–356

Comeau AM, Philippe B, Thaler M, Gosselin M, Poulin M, Lovejoy C (2013) Protists in Arctic drift and land-fast sea ice. J Phycol 49:229–240. doi:10.1111/jpy.12026

Cota G, Horne E (1989) Physical control of arctic ice algal production. Mar Ecol Prog Ser 52:111–121

Deming JW (2010) Sea ice bacteria and viruses. In: Thomas DN, Dieckmann GS (eds) Sea ice, 2nd edn. Wiley Blackwell Publishing, Malaysia, pp 248–282

Ducklow H (2000) Bacterial production and biomass in the oceans. In: Kirchman DL (ed) Microbial ecology of the oceans. Wiley, Liss, pp 85–120

Ducklow HW (2003) Seasonal production and bacterial utilization of DOC in the Ross Sea, Antarctica. Biogeochem of the Ross Sea 78:143–158. doi:10.1029/078ARS09

Falkowski PG, Owens TG (1978) Effects of light intensity on photosynthesis and dark respiration in six species of marine phytoplankton. Mar Biol 45:289–295

Glaz P, Sirois P, Archambault P, Nozais C (2014) Impact of forest harvesting on trophic structure of eastern Canadian boreal shield lakes: insights from stable isotope analyses. PLoS ONE. doi:10.1371/journal.pone.0096143

Golden KM, Ackley SF, Lytle VI (1998) The percolation phase transition in sea ice. Science 282(5397):2238–2241. doi:10.1126/science.282.5397.2238

Gosselin M, Legendre L, Demers S, Ingram RG (1985) Responses of sea-ice microalgae to climatic and fortnightly tidal energy inputs (Manitounuk Sound, Hudson bay). Can J Fish Aquat Sci 42:999–1006

Gosselin M, Levasseur M, Wheeler PA, Horner RA, Booth BC (1997) New measurements of phytoplankton and ice algal production in the Arctic ocean. Deep Sea Res II 44(8):1623–1644. doi:10.1016/S0967-0645(97)00054-4

Haecky P, Anderson A (1999) Primary and bacterial production in sea ice in the northern Baltic sea. Aquat Microb Ecol 20:107–118. doi:10.3354/ame020107

Hawes I, Lund-Hansen LC, Sorrell BK, Nielsen MH, Borźak R, Buss I (2012) Photobiology of sea ice algae during initial spring growth in Kangerlussuaq, West Greenland: insights from imaging variable chlorophyll fluorescence of ice cores. Photosynth Res 112:103–115. doi:10.1007/s11120-012-9736-7

He J, Inghong C, Iaodong JX, Bo C, Yong Y (2005) Characterization of the summer pack ice biotic community of Canada Basin. Acta Ocean Sin 24(6):80–87

Hezel PJ, Zhang X, Bitz CM, Kelly BP, Massonnet F (2012) Projected decline in spring snow depth on Arctic sea ice caused by progressively later autumn open ocean freeze-up this century. Geophys Res Lett 39:L17505. doi:10.1029/2012GL052794

Hsaio SIC (1992) Dynamics of ice algae and phytoplankton in Frobisher Bay. Polar Biol 12:645–651. doi:10.1007/BF00236987

Jackson JM, Allen SE, McLaughlin FA, Woodgate RA, Carmack EC (2011) Changes to the near-surface waters in the Canada Basin, Arctic Ocean from 1993–2009: a basin in transition. J Geophys Res. doi:10.1029/2011JC007069

Kaartokallio H, Søgaard DH, Norman L, Rysgaard S, Tison JL-, Delille B, Thomas DN (2013) Short-term variability in bacterial abundance, cell properties, and incorporation of leucine and thymidine in subarctic sea ice. Aquat Microbiol Ecol 71:57–73. doi:10.3354/ame01667

Kana TM (1990) Light-dependent oxygen cycling measured by an oxygen-18 isotope dilution technique. Mar Ecol Prog Ser 64:293–300

Kirchman DL (1993) Chapter 58: leucine incorporation as a measure of biomass production by heterotrophic bacteria. Handbook of methods in aquatic microbial ecology. CRC Press, Florida, pp 509–518

Kirchmann D (2001) Measuring bacterial biomass production and growth rates from leucine incorporation in natural aquatic environments. Marine Microbiol 30:227–237. doi:10.1016/S0580-9517(01)30047-8

Kirst GO, Wiencke C (1995) Ecophysiology of polar algae. J Phycol 31:181–199. doi:10.1111/j.0022-3646.1995.00181.x

Lee SH, Whiteledge TE, Kang S-H (2008) Spring time production of bottom ice algae in the landfast sea ice zone at Barrow Alaska. J Exp Mar Biol Ecol 367:204–212. doi:10.1016/j.jembe.2008.09.018

Legendre L, Demers S, Gosselin M (1987) Chlorophyll and photosynthetic efficiency of size-fractionated sea-ice microalgae (Hudson Bay, Canadian Arctic). Mar Ecol Prog Ser 40:199–203

Legendre L, Ackley SF, Dieckmann GS, Gullicksen B, Horner R, Hoshiai T, Melnikov IA, Reeburgh WS, Spindler M, Sullivan CW (1992) Ecology of sea ice biota: part 2. Global significance. Polar Biol 12:429–444

Leu E, Søreide JE, Hessen DO, Falk-Petersen S, Berge J (2011) Consequences of changing sea-ice cover for primary and secondary producers in the European Arctic shelf seas: timing, quantity, and quality. Prog Oceanogr 90:18–32. doi:10.1016/j.pocean.2011.02.004

Leu E, Mundy CJ, Assmy A, Campbell K, Gabrielsen TM, Gosselin M, Juul-Pedersen T, Gradinger R (2015) Arctic spring awakening—steering principles behind the phenology of vernal ice algae blooms. Prog Oceanogr 139:151–170. doi:10.1016/j.pocean.2015.07.012

Li WKW, McLaughlin FA, Lovejoy C, Carmack EC (2009) Smallest algae thrive as the Arctic Ocean freshens. Science 326:539. doi:10.1126/science.1179798

López-Sandoval DC, Fernández A, Marañón E (2011) Dissolved and particulate primary production along a longitudinal gradient in the Mediterranean Sea. Biogeosciences 8:815–825. doi:10.5194/bg-8-815-2011

Maranger R, Bird DF, Juniper SK (1994) Viral and bacterial dynamics in Arctic sea ice during the spring algal bloom near resolute, NWT, Canada. Mar Ecol Prog Ser 111:121–127

Maranger R, Vaqué D, Nguyen D, Hébert M-P, Lara E (2015) Pan-Arctic patterns of planktonic heterotrophic microbial abundance and processes: controlling factors and potential impacts of warming. Prog Oceanogr 139:221–232. doi:10.1016/j.pocean.2015.07.006

Medlin LK, Priddle J (1990) Polar marine diatoms. British Antarctic Survey, Cambridge

Melnikov IA, Kolosova EG, Welch HE, Zhitina LS (2002) Sea ice biological communities and nutrient dynamics in the Canada basin of the Arctic Ocean. Deep Sea Res I 49:1623–1649. doi:10.1016/S0967-0637(02)00042-0

Michel C, Legendre L, Ingram RG, Gosselin M, Levasseur M (1996) Carbon budget of sea-ice algae in spring: evidence of a significant transfer to zooplankton grazers. J Geophys Res 101(C8):18345–18360

Michel C, Nielsen TG, Nozais C, Gosselin M (2002) Significance of sedimentation and grazing by ice micro- and meiofauna for carbon cycling in annual sea ice (northern Baffin Bay). Aquat Microbiol Ecol 30:57–68. doi:10.3354/ame030057

Mikkelsen DM, Rysgaard S, Glud RN (2008) Microalgal composition and primary production in Arctic sea ice: a seasonal study from Kobbefjord (Kangerluarsunnguaq), west Greenland. Mar Ecol Prog Ser 368:65–74. doi:10.3354/meps07627

Miller CB, Wheeler PA (2012) Biological oceanography. Wiley Blackwell Publishing, Malaysia

Mock T, Meiners KM, Giesenhagen HC (1997) Bacteria in sea ice and underlying brackish water at 54″26′50″N (Baltic Sea, Kiel Bight). Mar Ecol Progr Ser 158:23–40. doi:10.3354/meps158023

Mundy CJ, Barber DG, Michel C (2005) Variability of snow and ice thermal, physical and optical properties pertinent to sea ice algae biomass during spring. J Mar Syst 58:107–120. doi:10.1016/j.jmarsys.2005.07.003

Mundy CJ, Gosselin M, Ehn JK, Belzile C, Poulin M, Alou E, Roy S, Hop H, Lessard S, Papakyriakou TN, Barber DG, Stewart J (2011) Characteristics of two distinct high-light acclimated algal communities during advanced stages of sea ice melt. Polar Biol 34:1869–1896. doi:10.1007/s00300-011-0998-x

Niemi A, Michel C, Hille K, Poulin M (2011) Protist assemblages in winter sea

ice: setting the stage for the spring ice algal bloom. Polar Biol 34:1803–1817. doi:10.1007/s00300-011-1059-1

Parsons TR, Maita Y, Lalli CM (1984) A manual of chemical and biological methods for seawater analysis. Pergamon, New York

Piwosz K, Wiktor JM, Niemi A, Tatarek A, Michel C (2013) Mesoscale distribution and functional diversity of picoeukaryotes in the first-year ice of the Canadian Arctic. ISME 7:1461–1471. doi:10.1038/ismej.2013.39

Pogorzelec NM, Mundy CJ, Findlay CR, Campbell K, Diaz A, Ehn JK, Rysgaard S, Gough K (2017) FTIR imaging analysis of cell content in sea-ice diatom taxa during a spring bloom in the lower Northwest passage of the Canadian Arctic. Mar Ecol Prog Ser 569:77–88. doi:10.3354/meps12088

Poulin M, Cardinal A (1982) Sea ice diatoms from Manitounuk Sound, southeastern Hudson Bay (Quebec, Canada). III. Cymbellaceae, Entomoneidaceae, Gomphonemataceae, and Nitzschiaceae. Can J Bot 61:107–118

Poulin M, Daugbjerg N, Gradinger R, Ilyash L, Ratkova T, Cvon Quillfeldt (2011) The pan-Arctic biodiversity of marine pelagic and sea-ice unicellular eukaryotes: a first-attempt assessment. Mar Biodivers 41:13–28. doi:10.1007/s12526-010-0058-8

Riedel A, Michel C, Poulin M, Lessard S (2003) Taxonomy and abundance of microalgae and protists at a first-year sea ice station near Resolute Bay, Nunavut, spring to early summer 2001. Fisheries and Oceans Canada: Canadian data report of hydrography and ocean sciences 159

Riedel A, Michel C, Gosselin M, LeBlanc B (2007) Grazing of large-sized bacteria by sea-ice heterotrophic protists on the Mackenzie shelf during the winter-spring transition. Aquat Microb Ecol 50:25–38. doi:10.3354/ame01155

Rózańska M, Gosselin M, Poulin M, Wiktor JM, Michel C (2009) Influence of environmental factors on the development of bottom ice protest communities during the winter-spring transition. Mar Ecol Prog Ser 386:43–59. doi:10.3354/meps08092

Różańska M, Poulin M, Gosselin M (2008) Protist entrapment in newly formed sea ice in the Coastal Arctic Ocean. J Mar Syst 74:887–901. doi:10.1016/j.jmarsys.2007.11.009

Rysgaard S, Glud RN (2004) Anaerobic N2 production in Arctic sea ice. Limnol Oceanogr 49:86–94. doi:10.4319/lo.2004.49.1.0086

Sarmiento JL, Gruber N (2006) Ocean biogeochemical dynamics. Princeton University Press, Princeton

Sherr EB, Sherr BF (1993) Preservation and storage of samples for enumeration of heterotrophic protists. In: Kemp PF, Sherr BF, Sherr EB, Cole JJ (eds) Current methods in aquatic microbial ecology. Lewis Publishers, New York, pp 207–212

Sime-Ngando T, Juniper SK, Demers S (1997) Ice-brine and planktonic microheterotrophs from Saroma-ko Lagoon, Hokkaido (Japan): quantitative importance and trophodynamics. J Mar Syst 11:149–161. doi:10.1016/S0924-7963(96)00035-8

Smith REH, Clement P (1990) Heterotrophic activity and bacterial productivity in assemblages in microbes from sea ice in the High Arctic. Polar Biol 10:351–357. doi:10.1007/BF00237822

Smith REH, Clement P, Cota GF (1989) Population dynamics of bacteria in Arctic sea ice. Microb Ecol 17:63–76

Søgaard DH, Kristensen M, Rysgaard S, Glud RN, Hansen PJ, Hilligsoe KM (2010) Autotrophic and heterotrophic activity in Arctic first-year sea ice: seasonal study from Malene Bight, SW Greenland. Mar Ecol Progr Ser 419:31–45. doi:10.3354/meps08845

Søgaard DH, Thomas DN, Rysgaard S, Glud RN, Norman L, Kaartokallio H, Juul-Pedersen-Juul T, Gelfius N-X (2013) The relative contributions of biological and abiotic processes to carbon dynamics in subarctic sea ice. Polar Biol 36(12):1761–1777. doi:10.1007/s00300-013-1396-3

Søreide J, leu E, Berge J, Graeve M, Falk-Petersen SF (2010) Timing of blooms, algal food quality and *Calanus glacialis* reproduction and growth in a changing

Arctic. Glob Change Biol. doi:10.1111/j.1365-2486.2010.02175.x

Strickland JD, Parsons TR (1972) A practical handbook of seawater analysis, 2nd edn. Bulletin Fisheries Research Board of Canada, Ottawa

Tomas CR (1997) Identifying marine phytoplankton. Academic Press, California

Tremblay G, Belzile C, Gosselin M, Poulin M, Roy S, Tremblay J-E (2009) Late summer phytoplankton distribution along a 3500 km transect in Canadian Arctic waters: strong numerical dominance by picoeukaryotes. Aquat Microbiol Ecol 54:55–70. doi:10.3354/ame01257

Tremblay J, Anderson LG, Matrai P, Coupel P, Bélanger S, Michel C, Reigstad M (2016) Global and regional drivers of nutrient supply, primary production and CO_2 drawdown in the changing Arctic Ocean. Progr Oceanogr 139:171–196. doi:10.1016/j.pocean.2015.08.009

vonQuillfedt CH, Hegseth EN, Johsen G, Sakshaug E, Syvertsen EE (2009) Ice algae. In: Sakshaug E, Johnsen G, Kavacs K (eds) Ecosystem Barents Sea. Pair Academic Press, Trondheim, pp 285–302

Wassmann P, Reigstad M (2011) Future Arctic Ocean seasonal ice zones and implications for pelagic-benthic coupling. Oceanography 24(3):220–231. doi:10.5670/oceanog.2011.74

Webster MA, Rigor IG, Nghiem SV, Kurtz NT, Farrell SL, Perovich DK, Sturm M (2014) Interdecadal changes in snow depth on Arctic sea ice. J Geophys Res Oceans 119:5395–5406. doi:10.1002/2014JC009985